Korean J. Chem. Eng., 34(6), 1882-1888 (2017)
DOI: 10.1007/s11814-017-0051-z

pISSN: 0256-1115
eISSN: 1975-7220

Study on the mechanism of desulfurization and denitrification catalyzed by TiO_2 in the combustion with biomass and coal

Shu-Qin Wang†, Ming-Zhu Liu, Li-Li Sun, and Wei-Liang Cheng†

School of Environmental Science and Engineering, North China Electric Power University, Baoding, Hebei 071003, P. R. China
(*Received 4 September 2016 • accepted 27 February 2017*)

Abstract−The effects of Ca/S molar ratio, catalyst type, catalyst dosage, temperature on desulfurization and denitrification efficiency were investigated in the coal-powder combustion with corn cobs as biomass. The thermal characteristics of Shanxi coal and corn cob blends with V-TiO_2 were evaluated by thermogravimetric analyzer. The catalytic mechanisms of V-TiO_2 on combustion, desulfurization and denitrification were discussed, suggesting that the mechanisms are in good agreement with the experimental data. The results show that the control parameters of the ideal desulfurization and denitrification efficiency should follow that the dosage of V-TiO_2 catalyst is 8% with a Ca/S ratio of 2.3 at a treatment temperature 850 °C. Meanwhile, the combustion efficiency could be effectively improved with the mixture of corn cob and V-TiO_2. The thermal characteristics of coal char and corn cob char blends with V-TiO_2 were evaluated using thermogravimetric analysis and derivative thermogravimetry methods to discuss the heterogeneous NO reduction mechanisms. The results show that the biomass chars were more active than coal chars in reducing NO, and the specific surface area of the chars was increased with V-TiO_2, which indicates that V-TiO_2 exhibits significant influence on catalytic combustion, desulfurization and denitrification.

Keywords: Biomass and Coal Co-combustion, Desulfurization, Denitrification, Doping TiO_2

INTRODUCTION

Energy storage and conversion systems have been receiving increasing attention globally due to the overwhelming energy consumption [1,2]. Among energy systems, biomass and coal co-combustion technology can be used in grate furnaces and fluidized bed combustion with various advantages, which can fulfill utilization of the huge investment and infrastructure of the existing coal power plants. The addition of biomass to coal combustion can reduce NO emissions. This behavior could be linked to the rapid combustion of HCN and NH_i of corn cob, which could favor the conversion of NO into N_2.

To date, communities have focused on the study of coal and biomass co-combustion, with most efforts on the combustion characteristics [3-7], influence factors [8,9] and emission characteristics of sulfur oxides and nitrogen oxides [10-13]. Ahn et al. analyzed the combustion characteristics of biomass and coal blends by using a thermogravimetric analyzer [8]. The results show that biomass has high reactivity in comparison with coal due to its large volatile matter content and low burnout temperature. Xie et al. studied the emission characteristics of SO_2, NO and N_2O in a bench scale circulating fluidized bed combustor for coal and biomass co-combustion [12], which revealed that increasing the biomass mass content during coal-biomass co-combustion can significantly decrease the emission of NO and N_2O, but increase SO_2 emission. Utilization of pyrolysis gas coupled with Ca-based absorbent additives to reduce the emissions of NO, N_2O and SO_2 simultaneously is still open to future discussion. Daood et al. reported that biomass and coal mixture with a small amount of additives, such as CaO, TiO_2 and Fe_2O_3, is capable of enhancing the volatile hydrocarbon cracking to facilitate both NO reduction and improve combustion of coal fired burners [14]. However, an ideal additive for combined desulfurization and denitrification is still under development.

At present, nano-TiO_2 has been widely used in air treatment due to its high catalytic activity and high stability [15,16]. The effects of nano-TiO_2 on the individual coal combustion efficiency, desulfurization and denitrification efficiency were studied in our previous work [17-19]. The results showed that nano-TiO_2 can effectively reduce NO_X emissions, and could catalyze the reaction of CaO desulfurization and coal combustion.

In this contribution, we investigated the characteristics of NO_x and SO_2 emission in coal-powder combustion with corn cob as biomass. The effect of doped TiO_2 on the desulfurization and denitrification efficiency of the biomass and coal co-combustion was investigated to determine the control parameters. The mechanism of catalytic combustion, CaO desulfurization and homogeneous NO reduction with the addition of V-TiO_2 was discussed, which promised a stage to provide theoretical base for control strategies to realize the boiler emission reduction.

MATERIALS AND METHODS

1. Experimental Materials

Pure TiO_2 nanoparticles were prepared via the sol-gel method

†To whom correspondence should be addressed.
E-mail: wsqhg@163.com, cheng_w_l@163.com
‡The paper will be reported in the 11th China-Korea Clean Energy Workshop.

Table 1. Chemical analysis of samples as Shanxi coal and Hebei corn cob

	Proximate analysis[ad] (wt%)				Ultimate analysis[ad] (wt%)				
	M	A	V	FC	C	H	O[b]	N	S
Shanxi coals	3.14	18.29	27.60	50.97	56.69	3.86	14.81	1.04	2.17
Hebei corn cobs	3.78	0.02	76.00	20.20	44.43	6.25	44.82	0.62	0.08

[ad]On air-dried basis

[b]Calculated by difference; M: moisture; A: ash; V: volatile matter; FC: fixed carbon

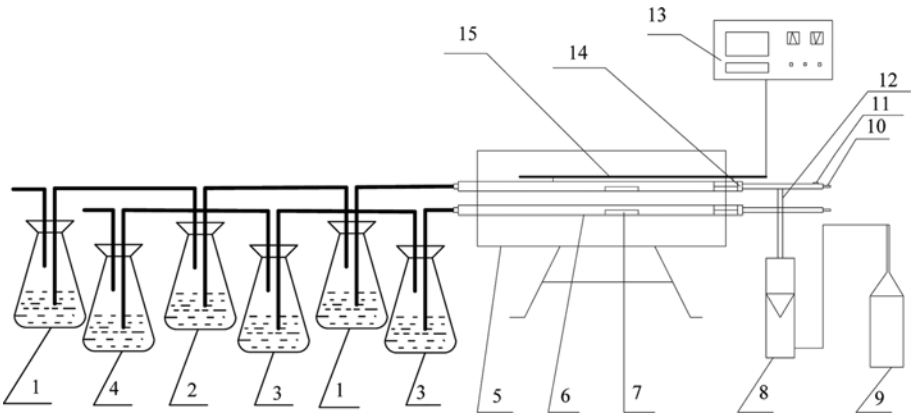

Fig. 1. The desulfurization and denitrification system of biomass and coal co-combustion.

1. NO_2 absorbing solution
2. Chromium oxide solution
3. Ammonium sulfamate and ammonium sulfate mixed solution
4. Lime solution
5. Combustion furnace
6. Combustion tube
7. Combustion boat
8. Flowmeter
9. Oxygen cylinder
10. Tipping cap
11. Push rod
12. T type tube
13. Temperature controller
14. Rubber plug
15. Thermocouple

using tetrabutyltitanate, glacial acetic acid, ethyl alcohol absolute and high pure water as the starting materials to get the sol. Then the dried sol was under microwave irradiation for 20 min. Finally, the dried gel obtained was calcined at 500 °C for 3 h to get the pure TiO_2 powder. To prepare doped TiO_2, the above procedure was repeated, adding different dopants, respectively. F-TiO_2, Mn-TiO_2 were calcined at 500 °C for 3 h and V-TiO_2 was calcined at 700 °C for 3 h. Both V_2O_5 and MnO_2 were analytical commercial catalysts.

A certain weight of Shanxi coal, Hebei corn cob, CaO and catalyst were measured and then mixed together thoroughly to prepare the experimental samples. The samples were defined as follows: sample A: Shanxi coal, sample B: Shanxi coal+Hebei corn cob, sample C: Shanxi coal+Hebei corn cob+CaO. The blending ratios of coal and corn cob of sample B, sample C were all 8 : 2. The proximate analysis (by GB/T212-2001) and ultimate analysis (by GB214/T-2007) of Shanxi coals and Hebei corn cobs are shown in Table 1.

2. Experimental Procedure

In the beginning of the experiments, a certain amount of experimental samples was transferred into a porcelain boat, following by positioning at the center of a tubular furnace. The experimental sample was heated to 500 °C for 5 min through oxygen gas flow, and then heated to different treatment temperatures, 750-900 °C, for 25 min until the completion of combustion process. The feed gas was supplied from oxygen gas cylinders with a volume flow at 40 mL/min.

SO_2 concentration was determined by iodometric method (HJ/T56-2000). The NO concentration was determined using naphthyl ethylenediamine dihydrochloride spectrophotometric method (HJ479-2009). The desulfurization and denitrification efficiencies were calculated by the concentration difference between the initial (coal combustion alone) and instant concentration.

The denitrification and desulfurization system of the biomass and coal blends is shown in Fig. 1.

Thermal characteristics of the samples (coals with corn cobs as well as coal chars with corn cob char blends) were studied by using thermal analyzer (STQ-600). During the analysis, sample weight was about 5.00 mg and heating rate was 180 °C/min. The air flow rate was at 60 mL/min in the first group, for which the effect of V-TiO_2 on the coal and biomass co-combustion was studied. The second in which the denitrification mechanism was discussed by the same method, but with NO flow instead of air flow.

RESULTS AND DISCUSSION

The XRD patterns of the V-TiO_2 (1%, 700 °C, 3 h) and pure TiO_2 (700 °C, 3 h) are shown in Fig. 2. The crystal structure of V-TiO_2 and pure TiO_2 was all mixed crystallinity constituted of anatase and rutile. The crystal size of the pure TiO_2 was 63.8 nm, while the crystal size changed to 30.9 nm with V doping. Also, the mixing peaks of V-TiO_2 were significantly reduced, indicating that the integrity of crystal phase structure of the V-doped TiO_2 was higher than that of the pure TiO_2. In addition, V-TiO_2 showed a higher surface area 6.6 $m^2\ g^{-1}$ with respect to the undoped TiO_2 (3.4 $m^2\ g^{-1}$), which is favorable for the adsorption of O_2. Therefore, the catalytic activity

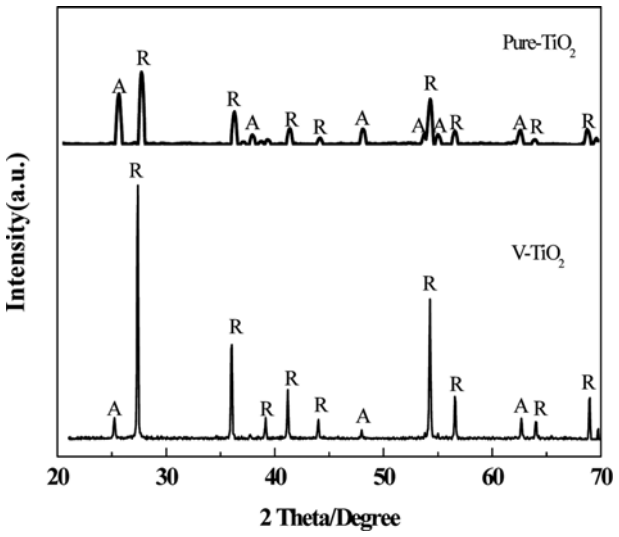

Fig. 2. XRD patterns of the pure TiO_2 (up) and V-TiO_2 (bottom); A-Anatase, R-Rutile.

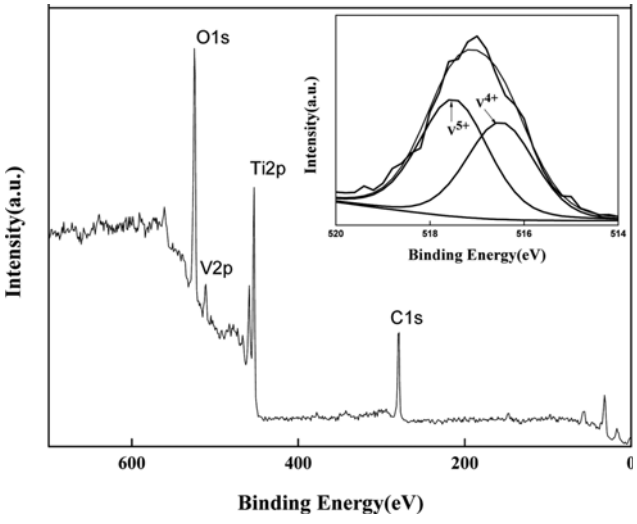

Fig. 3. XPS spectra of V-TiO_2.

of the TiO_2 was greatly improved with V doping.

As shown in Fig. 3, XPS analysis was used to investigate the chemical compositions and states of surface elements in the modified TiO_2. Fig. 3 shows that vanadium exists in the forms of V^{4+} and V^{5+} in the doped samples. However, the ionic radius of V^{4+} is very close to that of Ti^{4+}, and thus V^{4+} can be easily substituted for the

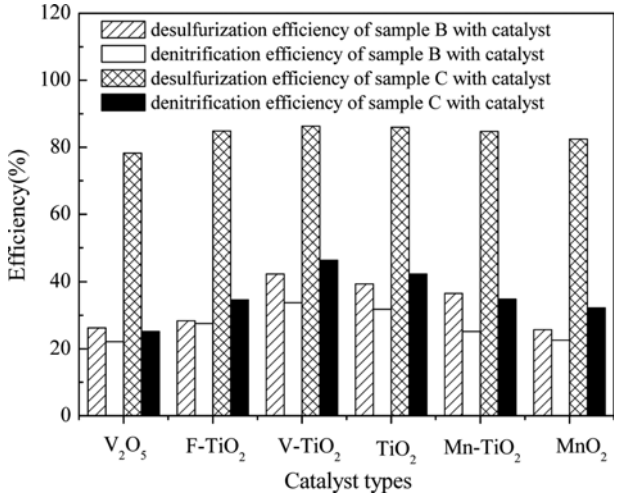

Fig. 4. Effect of catalyst on desulfurization and denitrification efficiency (temperature at 850 °C, Ca/S molar ratio of 2.3 and V-TiO_2 dosage ratio at 8%).

Ti^{4+} in the TiO_2 crystal lattice [20,21]. After V^{4+} substitution, the distance between Ti^{4+} and O^{2-} can be decreased, and the catalytic activity of the catalyst can be improved by O^{2-} [22].

1. Effect of Ca/S Molar Ratio on Desulfurization and Denitrification Efficiency

The effect of Ca/S molar ratio on desulfurization and denitrification efficiency of sample C with and without V-TiO_2 is shown in Table 2.

According to Table 2, the desulfurization efficiency increases with the increase of Ca/S ratio at beginning and approaches the maximum value when the Ca/S ratio is 2.3. Subsequently, the desulfurization efficiency decreases with the increase of Ca/S ratio. This observation is because excessive amount of CaO would be attached to the surface of the reactants, resulting in the thick product layer, thus increasing the difficulty of the diffusion of SO_2. The denitrification efficiency shows limited changes with the increase of Ca/S ratio, which suggests that CaO has no significant effect on the denitrification efficiency. Denitrification effect of sample C can be observed due to the addition of corn cobs. Biomass volatile fractions would fast precipitate to form coke with high porosity and activity, prompting NO_x decomposition [23]. Therefore, the Ca/S ratio for the ideal controllable desulfurization technology was determined to be 2.3.

2. Effect of Catalyst Types on Desulfurization and Denitrification Efficiency

The effect of catalyst type on desulfurization and denitrification

Table 2. Effect of Ca/S on desulfurization and denitrification efficiency (temperature at 850 °C with V-TiO_2 dosage ratio of 8%)

Efficiency (%)	Samples	Ca/S ratio				
		1.2	2.0	2.3	3	3.5
Desulfurization efficiency	Sample C	63.5	77.2	79.9	73.6	70.6
	Sample C with V-TiO_2	70.7	86.5	93.4	83.8	81.3
Denitrification efficiency	Sample C	21.7	20.9	20.6	20.3	20.0
	Sample C with V-TiO_2	43.2	43.4	46.6	41.2	39.0

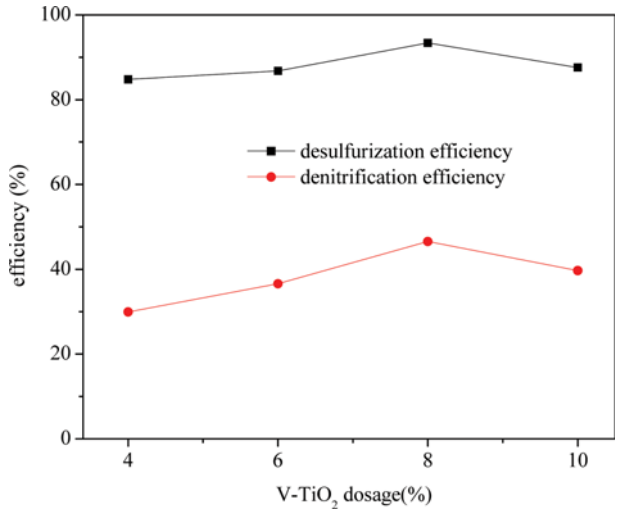

Fig. 5. Effect of V-TiO_2 dosage on desulfurization and denitrification efficiency (temperature at 850 °C and Ca/S ratio of 2.3).

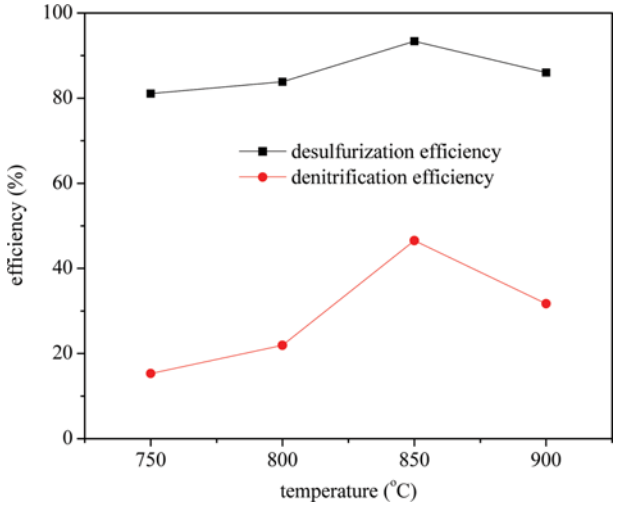

Fig. 6. Effect of temperature on desulfurization and denitrification efficiency (V-TiO_2 dosage at 8% and Ca/S ratio of 2.3).

efficiency with the same mass catalyst added is shown in Fig. 4. Samples with the addition of V-TiO_2 show the highest efficiency in desulfurization and denitrification. The relative molecular mass of TiO_2 is less than V_2O_5 and MnO_2, indicating that the molar mass of TiO_2 is bigger than V_2O_5 and MnO_2 with the same mass catalyst added. Therefore, the adsorption capacity is enhanced by the TiO_2 of larger specific surface area. The catalytic efficiency of TiO_2 can be enhanced with nonmetals or metal doping. Moreover, the doping element will also affect the catalytic properties. The radii of both V^{4+} (0.058 nm) and V^{5+} (0.054 nm) are smaller than that of Ti^{4+}, and therefore the V ions might easily enter the crystal lattice for substituting Ti^{4+} position. Consequently, V-TiO_2 shows higher catalytic activity than other modified TiO_2, and the corresponding analysis for the effect of V-TiO_2 was carried out in the following experiment.

3. Effect of V-TiO_2 Dosage on Desulfurization and Denitrification Efficiency

The effect of V-TiO_2 dosage on desulfurization and denitrification efficiency of sample C with V-TiO_2 is shown in Fig. 5. The desulfurization and denitrification efficiency increases with the increase of V-TiO_2 dosage at beginning and achieves the peak value when the V-TiO_2 dosage is 8%. This observation is probably because more active centers can be formed in the reaction surface with lower V-TiO_2 dosage, which is beneficial to the diffusion of SO_2, NO_x and heterogeneous reaction of SO_2, NO_x with CaO, thus improving the efficiency of desulfurization and denitrification. But if the dosage ratio of TiO_2 is higher than the optimal value, the additive will adhere to the surface of coal and block the surface pores. Meanwhile, the vanadium and titanium ions in V-TiO_2 can be combined with the oxygen functional groups in coals, which can also react with minerals in the coals [24], thus in turn suppressing the combustion.

4. Effect of Combustion Temperature on Desulfurization and Denitrification Efficiency

The desulfurization and denitrification efficiencies of sample C with V-TiO_2 at different temperatures are shown in Fig. 6. The optimal temperature for achieving high efficiency is 850 °C. This is mainly due to the sintering phenomenon of $CaSO_4$ at high temperature, which enables the deposition products to cover the entire local porosity, thus increasing the difficulty in SO_2 transfer. On the other hand, the chars fabricated at higher pyrolysis temperature have smaller specific surface area, fewer reactive sites and smaller amounts of active carbon to participate in the reaction with NO, which results in the decrease of NO conversion [25].

5. Effect of V-TiO_2 on the Coal and Biomass Co-combustion

We used thermogravimetric analysis (TG) and derivative thermogravimetry (DTG) to evaluate thermal characteristics. The TG curve and DTG curve were analyzed to determine the relevant combustion parameters, including ignition temperature, burnout temperature, maximum rate of mass loss and peak temperature. Ignition temperature is assigned to the temperature when weight loss first reaches 0.2%/min. Burnout temperature represents the temperature when the weight loss falls below 0.2%/min. The limit of 0.2%/min was established by using the actual profile as an arbitrary limit for the start and end of the peaks. Maximum rate of mass loss indicates the maximum reactivity attained in terms of rate of weight loss at DTG peak temperatures. The activation energy was calculated by Coats-Redfern method [26].

As shown in Table 3, ignition temperature, burnout temperature and activation energy of sample B are all lower than those of sample A due to the addition of corn cobs. The maximum rate of mass loss is considered directly proportional to the reactivity of the sample [27], which indicates that the corn cob mixture can improve combustion efficiency. All the biomass fuels have shown volatilization as the predominant combustion process. Then, biomass could release heat from the volatilization stage, which may play an important role in preheating and softening the structure of the fixed carbon [28], thereby promoting its combustion performance. Moreover, sample B with V-TiO_2 shows lower activation energy in comparison with sample B. Meanwhile, sample C with V-TiO_2 also shows lower activation energy, compared to sample C. Such observation could be understood by the fact that an active center will be formed

Table 3. Combustion reaction parameters

	Sample A	Sample B	Sample C	Sample B with V-TiO_2	Sample C with V-TiO_2
Ignition temperature (°C)	343	329	319	298	274
Burnout temperature (°C)	843	840	838	833	830
Maximum mass loss rate (%/min)	0.182	0.216	0.236	0.289	0.534
Peak temperature (°C)	834	823	815	810	795
Activation energy (kJ/mol)	72.6	67.8	65.6	54.4	48.0
R^2	0.9938	0.9974	0.9987	0.9994	0.9984

on the coal surface with the addition of V-TiO_2, which could accelerate the carbon oxidation and volatility, resulting in promoting the combustion reaction. Therefore, combustion performance can be improved by V-TiO_2 regardless of the addition of CaO.

6. Desulfurization Mechanism

Coal ash compositions were analyzed by X-ray fluorescence spectrometer ZSX100e (DZ/T0167-2006), where the content of SO_3 was analyzed by gravimetric method (GB/T1574-1995). The results show that CaO content of sample B with V-TiO_2 (3.84%) is less than that of sample B (4.54%), while SO_3 content of sample B with V-TiO_2 (5.67%) is higher than that of sample B (3.44%). Moreover, CaO content reduces from 13.61% to 9.84%, while the SO_3 content increases from 11% to 15.39% in the sample C added with V-TiO_2. These findings indicate that V-TiO_2 can catalyze the conversion of SO_2 to SO_3, and SO_3 can react with CaO to produce $CaSO_4$ rather than $CaSO_3$ in the oxidative atmosphere. In the process, V-TiO_2 could serve as an oxygen carrier for promoting oxygen transfer. As the oxygen transfer rate increases, sulfation of CaO could be accelerated in the presence of V-TiO_2 [29]. On the other hand, the addition of V-TiO_2 significantly increases the pore diameter and surface area of the ashes, which is helpful to the diffusion and reaction of SO_2 [30] and thus the desulphurization efficiency could increase. The catalytic mechanisms are in good agreement with the experimental data.

Table 4. The combustion reaction parameters of char

	Sample 1	Sample 2	Sample 3	Sample 4	Sample 5
Maximum rate of mass loss (%/min)	0.077	0.09	0.114	0.163	0.228
Peak temperature (°C)	842	836	834	828	817
Activation energy (kJ/mol)	47.2	40.3	41.2	37.8	33.6
R^2	0.9982	0.9993	0.9948	0.9931	0.9992

Table 5. The specific surface area of char

	Sample 1	Sample 2	Sample 3	Sample 4	Sample 5
Specific surface area (m^2/g)	5.52	5.92	7.88	10.43	21.03

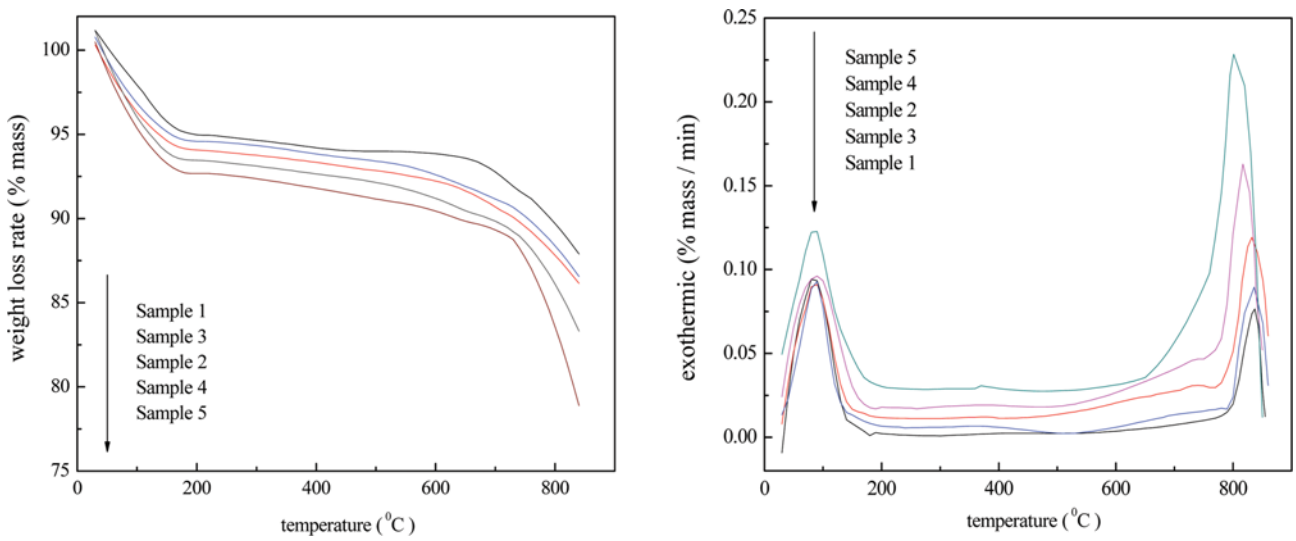

Fig. 7. TG curve of NO removal (up) and DTG curve of NO removal (bottom).

7. Denitrification Mechanism

Certain amounts of sample A, sample B, sample C, sample B with V-TiO_2, sample C with V-TiO_2 were separately transferred into the muffle furnace to prepare the char samples, assigned as sample 1, sample 2, sample 3, sample 4, and sample 5, respectively. The thermal characteristics of the samples were evaluated to investigate the heterogeneous NO-char reaction. Coats Redfern [26] method was used to calculate the activation energy, as listed in Table 4. Specific surface area of the chars was measured by a specific surface area analyzer (SA3100, Beckman Coulter, USA) and the results are shown in Table 5.

The maximum rate of mass loss of sample 2 is higher than that of sample 1, probably because biomass contains more alkali metals, and these metals may be associated with the organic matrix or bonded in the char particles, thus increasing the number of catalytic active sites leading to the biomass chars to be more active than coal chars in reducing NO [31]. Compared to sample 2, maximum rate of mass loss in sample 4 increases by 0.073%/min, and the activation energy in sample 4 reduces by 2.5 kJ/mol. Compared to sample 3, the maximum rate of mass loss in sample 5 increases by 0.114%/min, and the activation energy in sample 5 reduces by 7.6 kJ/mol. Such phenomenon is mainly linked to the fact that V-TiO_2 could provide active sites for char burning, which changes the pore distribution in the coal chars and in turn increases the specific surface area. The larger available specific surface area in the chars could lead to more effectiveness for NO reduction [32]. Therefore, the denitrification efficiency is greatly improved, consistent with the experimental data of denitrification.

CONCLUSIONS

The thermal characteristics of the coal powder and biomass mixture were evaluated with the presence of V-TiO_2 as catalyst, and the heterogeneous NO reduction mechanisms were discussed using TG and DTG. The major conclusions are below:

(1) The highest desulfurization and denitrification efficiencies should follow the controllable parameters, i.e., catalyst V-TiO_2 with dosage of 8%, Ca/S ratio of 2.3, combustion temperature at 850 °C. V-TiO_2 could catalyze the reaction of CaO desulfurization and NO removal.

(2) The characterizations of the samples show that the lattice distortion, higher surface area of TiO_2 and the unsaturated valences of V have been achieved. Meanwhile, the oxygen adsorbed on the catalyst surface results in forming the reactive oxygen species, and therefore the oxidation process of SO_2 and catalytic activity of TiO_2 have been greatly improved with V doping.

(3) The combustion efficiency could be effectively improved with the corn cob and V-TiO_2 mixture, and biomass chars are more active than coal chars in reducing NO.

(4) The combustion temperature at 850 °C consistent is with one of circulating fluidized bed boiler. The desulfurization agents, including CaO and catalyst V-TiO_2, can be directly applied to circulating fluidized bed boilers.

ACKNOWLEDGEMENTS

This work was financially supported by Beijing Natural Science Foundation (No. 3132017) and National Natural Science Foundation of China (No. 51476056).

REFERENCES

1. X. Y. Zhang, F. Hao, H. S. Chen and D. N. Fang, *J. Electrochem. Soc.*, **161**(14), A2243 (2014).
2. L.Yang, X. Zhang, Y. Li, F. Hao, H. Chen, M. Yang and D. Fang, *Electrochim. Acta*, **155**, 272 (2015).
3. M. V. Gil, D. Casal, C. Pevida, J. J. Pis and F. Rubiera, *Bioresour. Technol.*, **101**, 5601 (2010).
4. E. Lester, M. Gong and A. Thompson, *J. Anal. Appl. Pyrol.*, **80**, 111 (2007).
5. S. G. Sahu, P. Sarkar, N. Chakraborty and A. K. Adak, *Fuel Process. Technol.*, **91**, 369 (2010).
6. H. P. Wan, Y. H. Chang, W. C. Chien, H. T. Lee and C. C. Huang, *Fuel*, **87**, 761 (2008).
7. A. Kazagic and I. Smajevic, *Energy*, **32**, 2006 (2007).
8. S. Ahn, G. Choi and D. Kim, *Biomass Bioenergy*, **71**, 144 (2014).
9. X. Liu, M. Chen and Y. Wei, *Fuel*, **143**, 577 (2015).
10. J. Riaza, L. Álvarez, M. V. Gil, C. Pevida, J. J. Pis and F. Rubiera, *Energy Procedia*, **37**, 1405 (2013).
11. S. S. Daood, M. T. Javed, B. M. Gibbs and W. Nimmo, *Fuel*, **105**, 283 (2013).
12. J. J. Xie, X. M. Yang, L. Zhang, T. L. Ding, W. L. Song and W. G. Lin, *J. Environ. Sci.*, **19**, 109 (2007).
13. H. Liu, J. R. Qiu and X. W. Dong, *J. Eng. Therm. Energy Power*, **17**, 451 (2002).
14. S. S. Daood, G. Ord, T. Wilkinson and W. Nimmo, *Fuel*, **134**, 293 (2014).
15. Y. Yuan, J. Zhang, H. Li, Y. Li, Y. Zhao and C. Zheng, *Chem. Eng. J.*, **192**, 21 (2012).
16. Y. Zhao, J. Han, Y. Shao and Y. Feng, *Environ. Technol.*, **14**, 1555 (2009).
17. S. Q. Wang, Y. Zhao and D. D. Li, *J. Eng. Therm. Energy Power*, **23**, 50 (2008).
18. S. Q. Wang, Y. Zhao, Q. Tan and P. Y. Xu, *Environ. Sci.*, **29**, 518 (2008).
19. S. Q. Wang and H. Y. Kong, *J. N. China Electr. Power Univ.*, **3**, 79 (2008).
20. X. Zhang, L. Yang, F. Hao, H. Chen, M. Yang and D. Fang, *Nanomaterials*, **5**(4), 1985 (2015).
21. L. Li, C. Y. Liu and Y. Liu, *Mater. Chem. Phys.*, **113**, 551 (2009).
22. S. W. Ding, L. Li, X. W. Xu and L. Wu, *J. N. China Electr. Power Univ.*, **6**, 88 (2007).
23. L. Zhang, S. H. Zhang and X. H. Wang, *Power Syst. Eng.*, **23**, 127 (2007).
24. S. Q. Wang, C. R. Su and Y. Zhao, *J. N. China Electr. Power Univ.*, **5**, 89 (2011).
25. L. Dong, S. Gao, W. Song and G. Xu, *Fuel Process. Technol.*, **88**, 707 (2007).
26. J. Z. Liu, Z. G. Feng, B. S. Zhang, J. H. Zhou and K. F. Cen, *J. Power Eng.*, **26**, 121 (2006).
27. G. Zheng and J. A. Koziński, *Fuel*, **79**, 181 (2000).
28. J. Zhang, J. Li, Z. Hu, S. Yin, H. Zuo and B. Su, *Acta Energy Solaris Sinica*, **10**, 1847 (2013).

29. S. Q. Wang, Y. Zhao, P. P. Zhang and Y. D. Liu, *Chem. Eng. Res. Des.*, **89**, 1061 (2011).
30. Y. Zhao, S. Q. Wang, Y. Shen and X. Lu, *Energy*, **56**, 25 (2013).
31. L. Dong, S. Gao, W. Song and G. Xu, *Fuel Process. Technol.*, **88**, 707 (2007).
32. B. J. Zhong, W. W. Shi and W. B. Fu, *Fuel Process. Technol.*, **79**, 93 (2002).